The potential role of modern US in the follow-up of patients with retroperitoneal fibrosis

Lars Kamper, Alexander Sascha Brandt, Hendrik Ekamp, Matthias Hofer, Stephan Roth, Patrick Haage, Werner Piroth

PURPOSE
We aimed to evaluate a standardized ultrasonography (US) algorithm for the visualization of pathologic para-aortic tissue in retroperitoneal fibrosis (RPF).

MATERIALS AND METHODS
Thirty-five patients with lumbar RPF of typical extent, as determined by abdominal magnetic resonance imaging, were included. Examinations were conducted using standardized abdominal US with axial sections obtained at the levels of the renal arteries, aortic bifurcation, and both common iliac arteries. Imaging of each section was acquired with fundamental B-mode (US) and tissue harmonic imaging, respectively. In addition, we examined RPF visualized using extended field-of-view US.

RESULTS
Tissue harmonic imaging adequately visualized RPF of typical extent in 33 patients (94.2%). Excellent and good visualization with mild artifacts were achieved in 25 (71.4%) and six (17.1%) patients, respectively. When RPF spread along the iliac arteries, excellent visualization was achieved in 38.7% for the left side and 34.5% for the right side. There were significantly fewer diagnostic examinations for the right iliac (27.6%) than for the left one (9.7%) (P = 0.016). Overall, harmonic imaging achieved significantly better visualization than fundamental B-Mode (P < 0.001).

CONCLUSION
We described the first systematic evaluation of RPF visualization by modern US techniques. The best imaging quality was found in the typical RPF location, at the level of the aortic bifurcation. These results advocate for the presented US algorithm as an efficient follow-up alternative to cross-sectional imaging in RPF patients.

From the Departments of Diagnostic and Interventional Radiology (L.K. ✉ *lars.kamper@helios-kliniken.de*, H.E., P.H., W.P.), and Urology (A.S.B., S.R.), HELIOS Medical Center Wuppertal, University Hospital Witten/Herdecke, Wuppertal, Germany; the Dean`s Office (M.H.), Department of Medical Education, Heinrich-Heine University Medical Faculty, Duesseldorf, Germany

Chronic periaortitis or retroperitoneal fibrosis (RPF) is a rare fibrosing disease that affects para-aortic tissues (1–3). It typically presents as a proliferating lumbar process surrounding the ureters and retroperitoneal vascular structures (Fig. 1) (2, 4). Sporadic, atypical manifestations in pelvic and mesenteric regions are also possible (5).

Magnetic resonance imaging (MRI) allows precise evaluation of the extent and complications (6). RPF presents as hypointense (often isointense to striated muscle) plaques in native T1-weighted magnetic resonance (MR) images with significant gadolinium contrast enhancement of active and untreated retroperitoneal fibrosis (7–9).

Ultrasonography (US) is primarily used in patients with RPF for a rapid and practical diagnosis of consecutive hydronephrosis (6). RPF presents as a smooth-bordered mass with either an echo-poor or echo-free signal (10, 11). Two studies in the 1980s indicated that US revealed only a poor overall sensitivity in the detection of RPF (12, 13). Feinstein et al. (14) reported that only 25% of affected patients with computed tomography (CT)-mediated diagnosis of RPF showed corresponding ultrasonographic abnormalities. Since that time the quality of US scanners has improved dramatically, and modern techniques, such as tissue harmonic imaging (THI) and extended field-of-view US, have significant advantages for routine clinical diagnosis (15–17). Today, US has established itself as an effective and cost-efficient imaging method for the screening and follow-up of infrarenal aortic aneurysms (18, 19). US, however, is not used routinely for RPF follow-up, nor has a systematic evaluation of modern ultrasonographic methods been available to date.

The aim of the present study was to evaluate the potential role of modern ultrasonographic techniques for the visualization of fibrous tissue in patients with prediagnosed RPF.

Materials and methods

Study population

We examined a total of 56 consecutive patients already receiving medical therapy, or with newly diagnosed RPF disease. Only patients with RPF of the typical lumbar location were included in the analysis (Fig. 1). RPF extent was determined by abdominal MRI. Patients without delineable retroperitoneal soft tissue (n=15), or atypical suprarenal (n=1), and presacral (n=5) RPF location were excluded from the examination.

The resulting cohort of 35 patients consisted of 29 males and six females with a mean age of 56.1±10.4 years. Data storage and analysis conformed to the standards of the local ethics committee.

Imaging

Abdominal MR examinations were performed using a 1.5 Tesla scanner with a body array coil (Siemens Magnetom Avanto, Siemens Medical Systems, Erlangen, Germany). For the RPF extent evaluations, we used T1-weighted sequences with fat suppression before and after intravenously infused and weight-adapted gadoteridol contrast (ProHance, Bracco Imaging, Konstanz, Germany). Due to the potential risk of gadolinium-triggered nephrogenic systemic fibrosis (20), renal function was instead determined by serum creatinine and glomerular filtration rate (GFR). Patients with a GFR of 60–30 mL/min were informed of the increased risk, and no gadolinium-based contrast media were applied to patients with an estimated GFR of less than 30 mL/min.

Standardized US examinations were performed within 48 hours of the MR examination by three radiologists experienced in abdominal US. The examiners were not blinded to the RPF diagnosis or location. We used a high-end US scanner (ACUSON S2000, Siemens Medical Systems) and a "curved-array" abdominal transducer (3.5 MHz; frequency bandwidth, 1–4.5 MHz). We employed the installed abdominal presets with spatial real time compound imaging (SieClear, Siemens Medical Systems), and tissue-contrast-enhancement technology (DynamicTCE, Siemens Medical Systems) for enhanced contrast resolution and speckle reduction. Food restrictions and medication for bowel gas reduction were not prescribed prior to the examinations. All patients received a standardized examination guided by the abdominal vessels, which included axial sections at the levels of the renal arteries, aortic bifurcation, and both iliac vessels (Figs. 1c, 2). Imaging of each section was acquired with fundamental B-mode (US) and THI, respectively. In addition, we generated extended field-of-view US images of the infrarenal aorta and proximal iliac arteries using integrated software (SieScape, Siemens Medical Systems) in the cranio-caudal and caudo-cranial orientations. Panoramic imaging was performed under patient inspiration using the same "curved-array" abdominal transducer

with a frequency of 4 MHz, THI, and a mechanical index of 1.1–1.2. No color duplex techniques or US contrast agents were applied and no food restriction or anti-meteoristic medication was prescribed.

Image analyses and statistics

US and MR images were stored and analyzed in our picture archiving system (Centricity PACS, GE Healthcare, Milwaukee, Wisconsin, USA). All US images were analyzed in consensus by two radiologists experienced in abdominal US and MRI. We classified RPF visualization, if present, into four quality categories (Fig. 3): excellent (3), mild artifacts (2), significant artifacts (1),

and not diagnostic (0). If the RPF was not present in the actual section (e.g., cases without iliacal spreading), this was classified as not available (NA).

The overall visualization quality of THI and the fundamental B-mode was compared with Wilcoxon's rank-sum test. For comparison of the different ultrasonographic sections, we dichotomized the visualization result quality by not diagnostic/significant artifacts vs. mild artifacts/excellent visualization. We performed logistic regression analyses with repetitive reading to evaluate the dependence between visualization quality and the respective ultrasonographic section. Since we found significant differences in the global
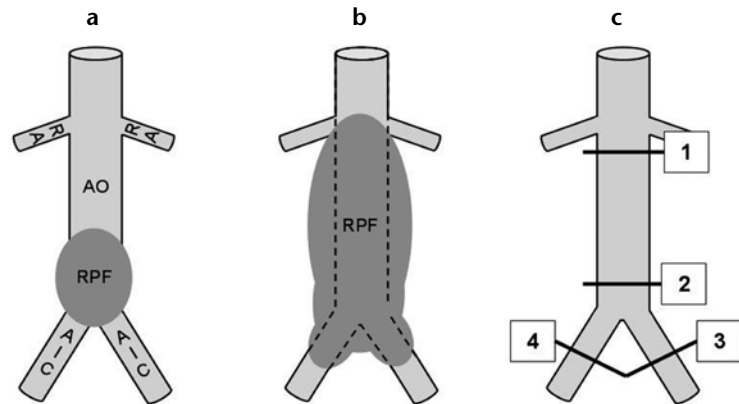
Figure 1. a–c. Typical extent of the retroperitoneal fibrosis surrounding the infrarenal aorta **(a)**. Spreading of the fibrosis to the renal arteries and along the common iliac arteries **(b)**. Standardized US examination with four transverse sections **(c)**. AO, aorta; AIC, common iliac artery; RA, renal artery; RPF, retroperitoneal fibrosis.
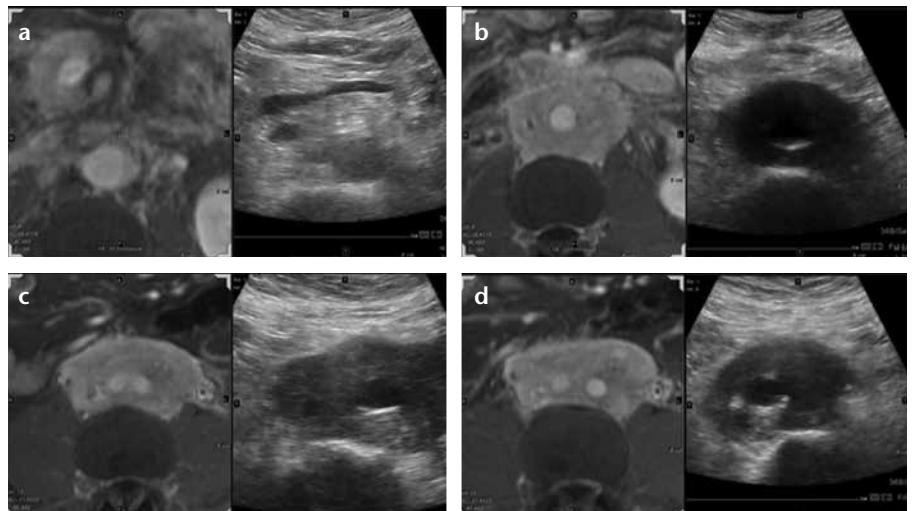
Figure 2. a–d. US sections with excellent visualization and corresponding MR images (T1-weighted with fat suppression) in a case with classical para-aortic retroperitoneal fibrosis location at the level of the renal arteries **(a)**, the bifurcation **(b)**, and both iliac arteries **(c, d)**. No para-aortic fibrosis was found at the level of the renal arteries **(a)**.

test, we performed additional pairwise comparisons of the different sections.

For all statistical analyses, P values <0.05 were considered to indicate significance. The extended field-of-view images were analyzed with respect to the continuity of generated panoramic images without artificial interruptions (Fig. 4).

Results

The RPF tissue displayed as a hypointense paravascular mass in T1-weighted MR images with distinct homogenous contrast enhancement (Fig. 2). According to the typical lumbar RPF location, we observed involvement of the aortic bifurcation in all 35 patients. Para-aortic RPF spreading to the level of the renal arteries was observed in 17 patients (48.5%). Iliac extent was found in 31 patients (88.6%) on the left, and in 29 patients (82.9%) on the right. Neither ventral aortic displacement nor additional retroperitoneal lymph nodes were observed in any patient.

In abdominal US examinations, the RPF presented as a hypoechogenic fusiform tissue formation surrounding the retroperitoneal vessels. Overall, ultrasonographic visualization was significantly better with THI than with US, per Wilcoxon's rank-sum test ($P <$ 0.001), regardless of the region examined. At the level of the aortic bifurcation, we achieved excellent visualization using THI in 25 patients (71.4%). We achieved good visualization with only mild artifacts in six patients (17.1%), and poor image quality with significant artifacts in two patients (5.7%). In all, diagnostic examination was achieved in 33 of 35 patients (94.2%), with no diagnostic visualization in only two patients (5.7%). In 17 patients with RPF extending to the renal arteries, we observed excellent or good visualization by THI in 13 patients (76.5%), and significant artifacts or no diagnostic visualization in four patients (23.5%). In cases with RPF spreading along the iliac arteries, excellent visualization was achieved for 38.7% for left-, and 34.5% for right-sided iliac extent. Examinations without diagnostic value were found in 9.7% for left- and 27.6% for right-iliac sections.

All THI and fundamental US examination results are shown in Table 1. We found the best visualization quality at the level of the aortic bifurcation with THI, and excellent quality in 71.4% of all examinations at the level of the renal arteries. Comparatively, fundamental US resulted in excellent quality in 47.1% of examinations. Iliac RPF visualization was of poorer quality compared to lumbar para-aortic visualization, regardless of the ultrasonographic method.

Table 2 shows the results of the categorized visualization qualities of THI and US. Comparison of the different ultrasonographic sections by logistic regression analysis revealed significant differences between the sections in the global test for both US ($P = 0.001$) and THI ($P = 0.011$).

The results of additional pairwise comparisons for specific ultrasonographic sections using a single method are shown in Table 3. In THI examinations, right iliac visualization was of
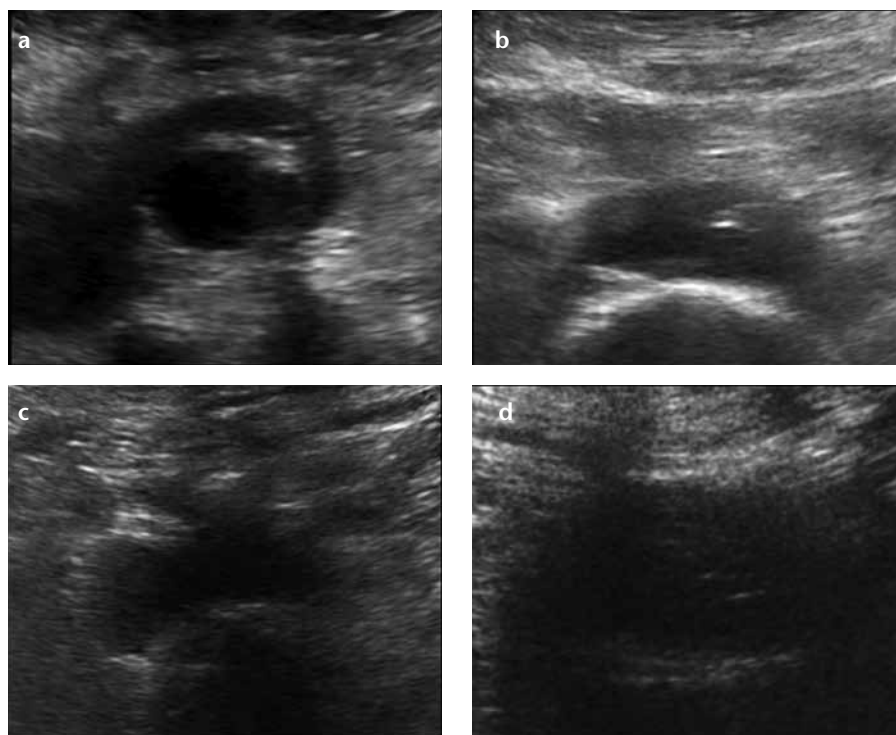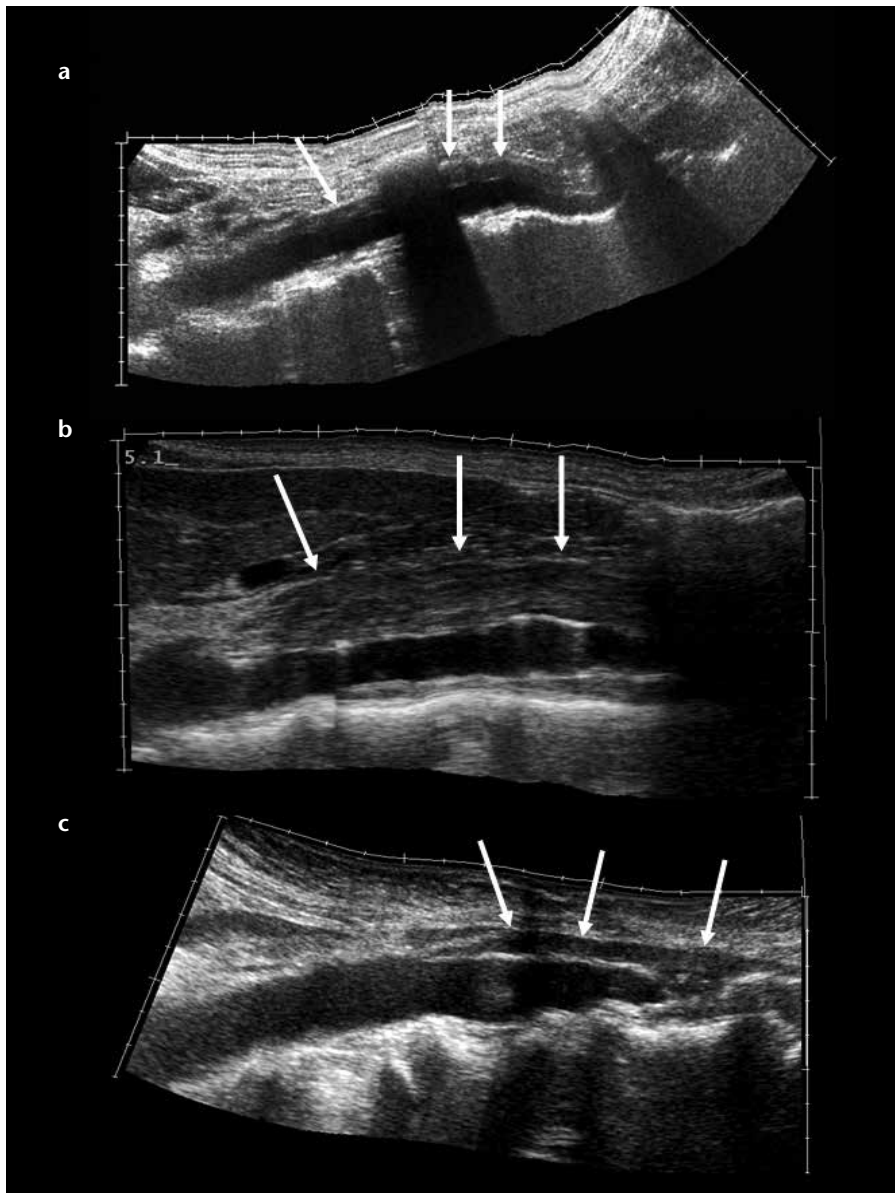

Figure 3. a–d. Retroperitoneal fibrosis visualization at the level of aortic bifurcation in excellent **(a)**, good **(b)**, poor **(c)**, and not diagnostic **(d)** quality.

Table 1. Quality of retroperitoneal fibrosis visualization with THI and B-mode (US)

	Renal arteries (n=17)		Aortic bifurcation (n=35)		Left iliac artery (n=31)		Right iliac artery (n=29)	
	THI	US	THI	US	THI	US	THI	US
Not diagnostic	2 (11.8%)	2 (11.8%)	2 (5.7%)	5 (14.3%)	3 (9.7%)	6 (19.4%)	8 (27.6%)	9 (31.0%)
Significant artifacts	2 (11.8%)	2 (11.8%)	2 (5.7%)	3 (8.6%)	7 (22.6%)	9 (29.0%)	9 (31.0%)	8 (27.6%)
Mild artifacts	2 (11.8%)	5 (29.4%)	6 (17.1%)	13 (37.1%)	9 (29.0%)	5 (16.1%)	2 (6.9%)	5 (17.2%)
Excellent	11 (64.7%)	8 (47.1%)	25 (71.4%)	14 (40.0%)	12 (38.7%)	11 (35.5%)	10 (34.5%)	7 (24.1%)

THI, tissue harmonic imaging; US, fundamental ultrasonography.

Figure 4. a–c. Retroperitoneal fibrosis visualization with extended field-of-view US. The *arrows* indicate the ventral border of the retroperitoneal fibrosis tissue. Continuous visualization with panorama image generation in the cranio-caudal direction **(a)**. Discontinuous retroperitoneal fibrosis visualization in the cranio-caudal direction **(b)**. Discontinuous retroperitoneal fibrosis visualization with panorama image generation in the caudo-cranial direction **(c)**.

Table 2. Categorized visualization qualities for THI and US in the different sections

	Renal arteries (n=17)	Aortic bifurcation (n=35)	Left iliac artery (n=31)	Right iliac artery (n=29)
THI				
Not diagnostic/significant artifacts	4 (23.5%)	4 (11.4%)	10 (32.3%)	17 (58.6%)
Mild artifacts/excellent visualization	13 (76.5%)	31 (88.6%)	21 (67.7%)	12 (41.4%)
US				
Not diagnostic/significant artifacts	4 (23.5%)	8 (22.9%)	15 (48.4%)	17 (58.6%)
Mild artifacts/excellent visualization	13 (76.5%)	27 (77.1%)	16 (51.6%)	12 (41.4%)

Global test by logistic regression analyses revealed significant differences between the respective sections for both THI ($P = 0.011$) and US ($P = 0.001$).
THI, tissue harmonic imaging; US, fundamental ultrasonography.

significantly lower quality than the left iliac RPF ($P = 0.016$, Table 2), whereas fundamental US revealed no significant differences between the iliac RPF visualizations ($P = 0.475$, Table 3).

In the extended field-of-view US analysis, we found continuously generated panoramic images without artificial interruptions in 22 patients (62.9%) for the cranio-caudal direction, and 13 patients (37.1%) for the caudo-cranial direction (Table 4). Excellent RPF visualization in the panoramic images was also achieved in 22 patients (62.9%) in the cranio-caudal direction and 20 patients (57.1%) in the caudo-cranial direction (Fig. 4). However, there was no overall significant difference in image quality between the directions.

Discussion

In this study, we present the first systematic evaluation of modern US techniques in the visualization of prediagnosed retroperitoneal fibrosis. Overall, RPF visualization was significantly better with THI compared to fundamental B-Mode ($P < 0.001$). Excellent RPF visualization was observed in 71.4% of patients, and good visualization with only mild artifacts in 17.1% of patients using THI.

US is an effective and cost-efficient imaging method for the screening and follow-up of infrarenal aortic aneurysms (18, 19). However, it is not routinely used for follow-up of para-aortic RPF. An examination of four patients with CT diagnosed RPF in the 1980s showed poor diagnostic sensitivity, with corresponding ultrasonographic findings in only one patient (14). To our knowledge, no state-of-the-art US technique evaluation in RPF exists to date. Published data consist primarily of case reports of one or only a few patients (21–23). Our data represent the first systematic evaluation of modern US techniques for RPF visualization. Compared to preceding studies with insufficient results (12–14), we observed significantly better results amounting to sufficient image quality in 94.2% of patients by THI imaging, and 85% using B-mode US. Our results correspond well to other abdominal US studies, such as those that evaluated detection of pancreatic (16) or renal (17) lesions. Image quality by THI was

Table 3. Pairwise comparison of the different sections for THI and B-mode (US)

	THI			US		
	Aortic bifurcation	Left iliac artery	Right iliac artery	Aortic bifurcation	Left iliac artery	Right iliac artery
Renal arteries	5.2 (0.4–62.4) $P = 0.198$	0.3 (0.3–2.7) $P = 0.263$	0.03 (0.0–0.5) $P = 0.013$	0.8 (0.1–4.6) $P = 0.772$	0.1 (0.02–0.7) $P = 0.018$	0.1 (0.0–0.4) $P = 0.005$
Aortic bifurcation	-	0.1 (0.01–0.7) $P = 0.023$	0.01 (0.0–0.2) $P = 0.001$	-	0.2 (0.0–0.6) $P = 0.009$	0.1 (0.0–0.4) $P = 0.002$
Left iliac artery	-	-	0.001 (0.0–0.3) $P = 0.016$	-	-	0.6 (0.2–2.3) $P = 0.475$

Data are given as odds ratio (95% confidence interval) and P values. $P < 0.05$ is considered as significant.
THI, tissue harmonic imaging; US, fundamental ultrasonography.

Table 4. Quality of RPF visualization with cranio-caudal and caudo-cranial generated panoramic US

	Cranio-caudal (n=35)	Caudo-cranial (n=35)
Continuous visualization	22 (62.9%)	13 (37.1%)
Not diagnostic	3 (8.6%)	5 (14.3%)
Significant artifacts	5 (14.3%)	2 (5.7%)
Mild artifacts	5 (14.3%)	8 (22.9%)
Excellent	22 (62.9%)	20 (57.1%)

significantly superior to fundamental B-mode. The best RPF visualization was achieved at the level of the aortic bifurcation, which is appropriate for typical RPF location (3, 5). We therefore conclude that the described US protocol can be used to visualize RPF in the typical lumbar location of patients known to have the disease. In patients with predominant iliac manifestation the US protocol is not recommended as it provides significantly lower visualization quality in the iliac location. As we employed nonblinded US examiners, these methods may not provide diagnostic sensitivity or specificity for patients with no RPF diagnosis.

Sagittal panoramic US revealed the fusiform character of the para-aortic tissue (Fig. 4); however, we observed numerous artifacts and discontinuous visualization of the RPF. Kim et al. (15) prospectively examined 31 patients using abdominal extended field-of-view US and found several potential benefits over fundamental B-mode US. These included better visualization of tubular abdominal structures, more accurate quantification of the large abdominal organs or associated lesions, and a documentation quality comparable to CT or MRI.

The response to medical treatment in RPF is based primarily on the regressive extent of the retroperitoneal fibrous tissue and clinical tests, such as regressive urinary obstruction (1). However, to date there is no standardized follow-up protocol. Acute-phase proteins, such as the C-reactive protein and erythrocyte sedimentation rate, are poor therapeutic success predictors (24). Therefore, cross-sectional abdominal imaging techniques (CT and MRI) are the basis of RPF location, extent, and follow-up evaluations (2–6). Abdominal CT is associated with iodinated contrast media and significant radiation, especially in repeated control examinations. MRI provides a better contrast to the surrounding retroperitoneal tissue without radiation exposure, but includes potential contraindications (e.g., implanted cardiac pacemakers) and is not always accessible. In addition, MRI in combination with intravenous gadolinium delivery has the added risk of inducing nephrogenic systemic fibrosis, especially in patients with impaired renal function. This is frequent in patients with RPF-triggered hydronephrosis, due to urethral obstruction.

Classical limitations of abdominal extended field-of-view US include movement artifacts and the superimposition of bowel gas (25). Both limitations may explain the rate of discontinuous panoramic images in our study, which did not differ between the cranio-caudal and caudo-cranial directions. Consequently, panoramic US does not provide additional diagnostic information in RPF patients. No food restriction or antimeteoristic medication was prescribed, as positive effects on image quality have been reported for only the upper abdominal regions (e.g., the biliary tract and gallbladder) (26–28). However, the reduced image quality for right-iliac-RPF visualization may be caused by caecal gas interposition.

One major limitation of the current study is the assessment of ultrasonographic image quality by the consensus of two radiologists without evaluation of the interobserver agreement. Further limitations include the lack of observer-blindness regarding disease status and MRI results; this may have resulted in overestimation of the validity and reliability of this study.

In conclusion, US with THI may be a cost-efficient alternative follow-up technique in a select group of patients known to have RPF in the typical lumbar location. The results suggest that US RPF visualization may be an effective supplement to classical follow-up US parameters, such as hydronephrosis. Additional research is necessary to evaluate the diagnostic potential of US protocols in patients whose RPF status is unknown.

Conflict of interest disclosure

References

al. Retroperitonele fibrose. Aktuelle Urologie 2007; 38:221–231. [CrossRef]

2. Cronin CG, Lohan DG, Blake MA, Roche C, McCarthy P, Murphy JM. Retroperitoneal fibrosis: a review of clinical features and imaging findings. Am J Roentgenol 2008; 191:423–431. [CrossRef]

3. Vaglio A, Salvarani C, Buzio C. Retroperitoneal fibrosis. Lancet 2006; 367:241–251. [CrossRef]

4. Amis ES Jr. Retroperitoneal fibrosis. Am J Roentgenol 1991; 157:321–329. [CrossRef]

5. Vivas I, Nicolás AI, Velázquez P, Elduayen B, Fernández-Villa T, Martínez-Cuesta A. Retroperitoneal fibrosis: typical and atypical manifestations. Br J Radiol 2000; 73:214–222.

6. Heckmann M, Uder M, Kuefner MA, Heinrich MC. Ormond's disease or secondary retroperitoneal fibrosis? An overview of retroperitoneal fibrosis. Rofo 2009; 181:317–323. [CrossRef]

7. Burn PR, Singh S, Barbar S, Boustead G, King CM. Role of gadolinium-enhanced magnetic resonance imaging in retroperitoneal fibrosis. Can Assoc Radiol J 2002; 53:168–170.

8. Geoghegan T, Byrne AT, Benfayed W, McAuley G, Torreggiani WC. Imaging and intervention of retroperitoneal fibrosis. Australas Radiol 2007; 51:26–34. [CrossRef]

9. Kamper L, Brandt AS, Scharwächter C, et al. MR evaluation of retroperitoneal fibrosis. Fortschr Roentgenstr 2011; 183:721-726. [CrossRef]

10. Bowie JD, Bernstein JR. Retroperitoneal fibrosis: ultrasound findings and case report. J Clin Ultrasound 1976; 4:435–437.

11. Fagan CJ, Larrieu AJ, Amparo EG. Retroperitoneal fibrosis: ultrasound and CT features. Am J Roentgenol 1979; 133:239–243. [CrossRef]

12. Doolin EJ, Goldstein H, Kessler B, Vinocur C, Marchildon MB. Familial retroperitoneal fibrosis. J Pediatr Surg 1987; 22:1092–1094. [CrossRef]

13. Sanders RC, Duffy T, Mcloughlin MG, Walsh PC. Sonography in the diagnosis of retroperitoneal fibrosis. J Urol 1977; 118:944–946.

14. Feinstein RS, Gatewood OM, Goldman SM, et al. Computerized tomography in the diagnosis of retroperitoneal fibrosis. J Urol 1981; 126:255–259.

15. Kim SH, Choi BI, Kim KW, et al. Extended field-of-view sonography: advantages in abdominal applications. J Ultrasound Med 2003; 2:385–394.

16. Hohl C, Schmidt T, Haage P, et al. Phase-inversion tissue harmonic imaging compared with conventional B-mode ultrasound in the evaluation of pancreatic lesions. Eur Radiol 2004; 14:1109–1117. [CrossRef]

17. Schmidt T, Hohl C, Haage P, et al. Diagnostic accuracy of phase-inversion tissue harmonic imaging versus fundamental B-mode sonography in the evaluation of focal lesions of the kidney. Am J Roentgenol 2003; 180:1639–1647. [CrossRef]

18. Manning BJ, O'Neill SM, Haider SN, Colgan MP, Madhavan P, Moore DJ. Duplex ultrasound in aneurysm surveillance following endovascular aneurysm repair: a comparison with computed tomography aortography. J Vasc Surg 2009; 49:60–65. [CrossRef]

19. Schuster H, Dünser E, Osinger K, et al. Ultrasound imaging of abdominal aortic aneurysms: diagnosis of aneurysms and complications and follow-up after endovascular repair. Ultraschall Med 2009; 30:528–543. [CrossRef]

20. Heinrich M, Uder M. Nephrogenic systemic fibrosis after application of gadolinium-based contrast agents--a status paper. Fortschr Roentgenstr 2007; 179:613–617. [CrossRef]

21. Moussavian B, Horrow MM. Retroperitoneal fibrosis. Ultrasound Q 2009; 25:89–91. [CrossRef]

22. Kamper L, Brandt AS, Winkler SB, et al. Imaging of retroperitoneal fibrosis. Med Klin (Munich) 2010; 105:582–584. [CrossRef]

23. Das CJ, Sharma R, Jain TP, Rai V, Chumber S, Das AK. Unusual appearance of retroperitoneal fibrosis simulating a tumour. Br J Radiol 2006; 79:e137–139. [CrossRef]

24. Magrey MN, Husni ME, Kushner I, Calabrese LH. Do acute-phase reactants predict response to glucocorticoid therapy in retroperitoneal fibrosis? Arthritis Rheum 2009; 61:674–679. [CrossRef]

25. Von Herbay A, Vogt C, Haussinger D. New methods in abdominal ultrasound: do they have a clinical value? Panoramic imaging, harmonic imaging technologies and contrast medium enhanced ultrasound. Z Gastroenterol 2001; 39:295–304. [CrossRef]

26. Dinkel E, Dittrich M, Peters H, Baumann W. Real-time ultrasound in Crohn's disease: characteristic features and clinical implications. Pediatr Radiol 1986; 16:8–12. [CrossRef]

27. Windler EE, Lempp FL. US of the upper abdomen: factors influencing image quality. Radiology 1985; 157:513–515.

28. Ehrenstein BP, Froh S, Schlottmann K, Schölmerich J, Schacherer D. To eat or not to eat? Effect of fasting prior to abdominal sonography examinations on the quality of imaging under routine conditions: a randomized, examiner-blinded trial. Scand J Gastroenterol 2009; 44:1048–1054. [CrossRef]